

# The nonlinear viscoelastic behavior of polypropylene

Aleksey D. Drozdov\*and Jesper deClaville Christiansen

Department of Production

Aalborg University

Fibigerstraede 16

DK-9220 Aalborg, Denmark

## Abstract

A series of tensile relaxation tests is performed on isotactic polypropylene in the sub-yield and post-yield regions at room temperature. Constitutive equations are derived for the time-dependent response of a semicrystalline polymer at isothermal loading with small strains. Adjustable parameters in the stress-strain relations are found by fitting experimental data. It is demonstrated that the growth of the longitudinal strain results in an increase in the relaxation rate in a small interval of strains in the sub-yield domain. When the strain exceeds some critical value which is substantially less than the apparent yield strain, the relaxation process becomes strain-independent.

---

\*Corresponding author

# 1 Introduction

This paper is concerned with the nonlinear viscoelastic behavior of semicrystalline polymers at isothermal uniaxial deformation with small strains. The study concentrates on the time-dependent response of isotactic polypropylene at room temperature, but we believe that the constitutive equations to be derived may be applied to other semicrystalline polymers [polyamides, polyethylene, polytetrafluorethylene, poly(ethylene terephthalate), poly(butylene terephthalate), poly(ethylene-2,6-naphthalene dicarboxylate), etc.] at temperatures above the glass transition point for the amorphous phase. The viscoelastic and viscoplastic behavior of polypropylene (PP) has been a focus of attention in the past decade, which may be explained by numerous applications of this material in industry (oriented films for packaging, reinforcing fibres, nonwoven fabrics, polyethylene–polypropylene copolymers, blends of PP with thermoplastic elastomers, etc.).

The nonlinear viscoelastic response of polypropylene was studied by Ward and Wolfe [1], see also [2], and Smart and Williams [3] three decades ago, and, more recently, by Ariyama [4, 5, 6, 7], Wortmann and Schulz [8, 9], Dutta and Edward [10], and Read and Tomlins [11]. In the past couple of years, the linear viscoelastic behavior of PP fibres was analyzed by Andreassen [12] and Lopez-Manchado and Arroyo [13], and the dynamic viscoelastic response of blends of isotactic polypropylene with polyethylene and styrene-butadiene-styrene triblock copolymer was studied by Souza and Demarquette [14] and Gallego Ferrer et al. [15], respectively. It was found that the loss tangent of isotactic polypropylene demonstrates two pronounced maxima being plotted versus temperature. The first maximum ( $\beta$ -transition in the interval between  $T = -20$  and  $T = 10$  °C) is associated with the glass transition in the most mobile part of the amorphous phase, whereas the other maximum ( $\alpha$ -transition in the interval between  $T = 50$  and  $T = 80$  °C) is attributed to the glass transition in the remaining part of the amorphous phase. This conclusion is confirmed by DSC (differential scanning calorimetry) traces for quenched PP that reveal an endotherm at  $T = 70$  °C which can be ascribed to thermal activation of amorphous regions with restricted mobility under heating [16].

Scanning electron microscopy and atomic force microscopy evidence that isotactic PP is a semicrystalline polymer with a complicated morphology. The crystalline phase contains brittle monoclinic  $\alpha$  spherulites (the characteristic size of  $100\text{ }\mu\text{m}$ ) consisting of crystalline lamellae (10 to 20 nm in thickness) directed in radial and tangential directions [17], and ductile hexagonal  $\beta$  spherulites consisting of parallel-stacked lamellae [18]. The amorphous phase is located between spherulites and inside the spherulites between lamellae. It consists of (i) relatively mobile chains between spherulites and between radial lamellae and (ii) severely restricted chains in regions bounded by radial and tangential lamellae. Mechanical loading results in inter-lamellar separation, rotation and twist of lamellae, fine and coarse slip of lamellar blocks, and their fragmentation. The latter leads to reorganization of blocks and strain-induced smectic–monoclinic transitions [16]. Straining of polypropylene causes chain slip through the crystals, breakage and reformation of tie chains, and activation of restricted amorphous regions driven by lamellar disintegration. In the post-yield region, these transformations of microstructure lead to the onset of voids between lamellae, break-up of crystals, and formation of fibrills [19].

It is hard to believe that these changes in the internal structure of PP may be ade-

quately described by a constitutive model with a relatively small number of adjustable parameters. To develop stress-strain relations for polypropylene, we apply the method of “homogenization of micro-structure” [20]. According to this approach, an individual (equivalent) phase is taken into account whose deformation captures essential features of the response of a semicrystalline polymer with a sophisticated morphology.

An amorphous phase is chosen as the equivalent phase because of the following reasons:

1. The viscoelastic response of semicrystalline polymers is conventionally associated with rearrangement of chains in amorphous regions [17].
2. According to the Takayanagi–Nitta concept [21, 22], sliding of tie chains along and their detachment from lamellae play the key role in the time-dependent response of semicrystalline polymers.
3. The viscoplastic flow in semicrystalline polymers is assumed to be “initiated in the amorphous phase before transitioning into the crystalline phase” [23],
4. Conventional models for polyethylene [20], polypropylene [24, 25] and poly(ethylene terephthalate) [26, 27] treat these polymers as networks of macromolecules.

Above the glass transition temperature for the mobile amorphous phase, polypropylene is thought of as a network of chains connected by junctions. Deformation of a specimen induces slip of junctions with respect to the bulk material. Sliding of junctions reflects slippage of tie molecules along lamellae and fine slip of lamellar blocks which are associated with the viscoplastic behavior of a semicrystalline polymer.

The viscoelastic response of PP is described in terms of the concent of transient networks [28, 29, 30, 31], and it is modelled as separation of active chains from their junctions and attachment of dangling chains to temporary nodes. Unlike previous studies, the network of polymeric chains is assumed to be strongly inhomogeneous, and it is treated as an ensemble of meso-regions (MR) with various potential energies for the detachment of active strands. Two types of MRs are distinguished: (i) active domains where strands separate from junctions as they are thermally agitated (these MRs model a mobile part of the amorphous phase), and (ii) passive domains where detachment of chains from junctions is prevented (these MRs reflect a part of the amorphous phase whose mobility is severely restricted by radial and tangential lamellae). Detachment of active chains from the network is treated as a thermally-activated process whose rate is given by the Eyring formula [32] with a strain-dependent attempt rate. Deformation of a specimen results in (i) an increase in the concentration of active MRs (which is ascribed to a partial release of the amorphous phase in passive meso-domains driven by fragmentation of lamellae) and (ii) a mechanically-induced acceleration of separation of strands from their junctions in active MRs.

An increase in the rate of relaxation of amorphous glassy polymers at straining is conventionally assumed to occur in the entire region of nonlinear viscoelasticity (from the strain  $\epsilon$  of at least 0.005 to the yield strain  $\epsilon_y$ ), see [33]. It is ascribed to the mechanically-induced growth of “free volume” between macromolecules which results in an increase in their mobility [34, 35, 36, 37]. Despite wide applications of the free volume concept in nonlinear viscoelasticity of solid polymers, experimental verification of this approach was

limited to relatively small strains (substantially below the yield point). The objectives of this study are (i) to report experimental data in tensile relaxation tests on isotactic polypropylene in the range of strains between  $\epsilon = 0.005$  (which corresponds to the end of the region of linear viscoelasticity) and  $\epsilon = 0.16$  (at higher strains necking of specimens is observed at the chosen cross-head speed), (ii) to derive constitutive equations for the time-dependent behavior of semicrystalline polymers at isothermal uniaxial stretching with small strains, (iii) to find adjustable parameters in the stress–strain relations by fitting observations, and (iv) to assess the interval of strains where the rate of relaxation monotonically increases with strain intensity.

The exposition is organized as follows. Section 2 is concerned with the description of the experimental procedure. Kinetic equations for sliding of junctions and detachment of active strands and attachment of dangling strands in active MRs are developed in Section 3. The strain energy density of a semicrystalline polymer is determined in Section 4. In Section 5 stress–strain relations are derived for uniaxial deformation of a specimen by using the laws of thermodynamics. These constitutive equations are employed to fit experimental data in tensile relaxation tests in Section 6. Some concluding remarks are formulated in Section 7.

## 2 Experimental procedure

A series of uniaxial tensile relaxation tests on polypropylene specimens was performed at room temperature. Isotactic polypropylene (Novolen 1100L) was supplied by Targor (BASF). ASTM dumbbell specimens with length 14.8 mm, width 10 mm and height 3.8 mm were injection molded and used without any thermal pre-treatment. Our DSC measurements (the sample mass 16.43 mg, the heating rate 10 K/min) demonstrated the specific enthalpy of melting  $\Delta H_m = 95.5$  J/g, which corresponds to the degree of crystallinity  $\kappa_c = 0.46$  (with reference to [38], the enthalpy of fusion for a fully crystalline polypropylene is assumed to be 209 J/g).

Mechanical experiments were performed with a testing machine Instron–5568 equipped with electro-mechanical sensors for the control of longitudinal strains in the active zone of samples (the distance between clips was about 50 mm). The tensile force was measured by the standard loading cell. The engineering stress  $\sigma$  was determined as the ratio of the axial force to the cross-sectional area of the specimens in the stress-free state (38 mm<sup>2</sup>).

16 relaxation tests were carried out at longitudinal strains in the range from  $\epsilon_1 = 0.005$  to  $\epsilon_{16} = 0.16$ , which correspond to the domain of nonlinear viscoelasticity, sub-yield and post-yield regions for isotactic polypropylene (the yield strain,  $\epsilon_y$ , is estimated by the supplier as 0.13).

Any relaxation test was performed on a new sample. No necking of specimens was observed in experiments. In the  $k$ th relaxation test ( $k = 1, \dots, 16$ ), a specimen was loaded with the constant cross-head speed 5 mm/min (which roughly corresponded to the strain rate  $\dot{\epsilon}_0 = 0.05$  min<sup>−1</sup>) up to the longitudinal strain  $\epsilon_k$ , which was preserved constant during the relaxation time  $t_r = 20$  min. The engineering stresses,  $\sigma$ , at the beginnings of relaxation tests are plotted in Figure 1 together with the stress–strain curve for the specimen strained up to  $\epsilon_{16} = 0.16$ . The figure demonstrates fair repeatability of

experimental data.

The longitudinal stress,  $\sigma$ , is plotted versus the logarithm ( $\log = \log_{10}$ ) of time  $t$  (the initial instant  $t = 0$  corresponds to the beginning of the relaxation process) in Figures 2 to 4. These figures show that the stress,  $\sigma$ , monotonically increases with strain,  $\epsilon$ , up to  $\epsilon_0 = 0.08$  and remains practically constant when the strain exceeds the critical strain  $\epsilon_0$ .

### 3 A micro-mechanical model

A semicrystalline polymer is treated as a temporary network of chains bridged by junctions. The network is modelled as an ensemble of meso-regions with various strengths of interaction between macromolecules. Two types of meso-domains are distinguished: passive and active. In passive MRs restricted by radial and tangential lamellae, inter-chain interaction prevents detachment of chains from junctions, which implies that all nodes in these domains are thought of as permanent. In active MRs, active strands (whose ends are connected to contiguous junctions) separate from temporary junctions at random times when these strands are thermally agitated. An active chain whose end slips from a junction is transformed into a dangling chain. A dangling chain returns into the active state when its free end captures a nearby junction at a random instant.

Denote by  $X$  the average number of active strands per unit mass of a polymer. Let  $X_a$  be the number of strands merged with the network in active MRs, and  $X_p$  the number of strands connected to the network in passive MRs. Under stretching some crystalline lamellae (that restrict mobility of chains in passive MRs) break, which results in the growth of the number of strands to be rearranged. As a consequence, the number of strands in active MRs increases and the number of strands in passive meso-domains decreases. This implies that the quantities  $X_a$  and  $X_p$  become functions of the current strain,  $\epsilon$ , which obey the conservation law

$$X_a(\epsilon) + X_p(\epsilon) = X. \quad (1)$$

Separation of active strands from the network and reformation of dangling strands in active MRs are thought of as thermally activated processes. It is assumed that detachment of active strands from their junctions is governed by the Eyring equation [32], where different meso-domains are characterized by different activation energies,  $\bar{\omega}$ , for separation of active strands from the network.

According to the theory of thermally-activated processes, the rate of separation of active strands in a MR with potential energy  $\bar{\omega}$  in the stress-free state is given by

$$\Gamma = \Gamma_a \exp\left(-\frac{\bar{\omega}}{k_B T}\right),$$

where  $k_B$  is Boltzmann's constant,  $T$  is the absolute temperature, and the pre-factor  $\Gamma_a$  is independent of energy  $\bar{\omega}$  and temperature  $T$ . Introducing the dimensionless potential energy

$$\omega = \frac{\bar{\omega}}{k_B T_0},$$

where  $T_0$  is some reference temperature, and disregarding the effects of small increments of temperature,  $\Delta T = T - T_0$ , on the rate of detachment,  $\Gamma$ , we arrive at the formula

$$\Gamma = \Gamma_a \exp(-\omega). \quad (2)$$

It is assumed that Eq. (2) is satisfied for an arbitrary loading process, provided that the attempt rate,  $\Gamma_a$ , is a function of the current strain,

$$\Gamma_a = \Gamma_a(\epsilon).$$

The distribution of active MRs with various potential energies is described by the probability density  $p(\omega)$  that equals the ratio of the number,  $N_a(\epsilon, \omega)$ , of active meso-domains with energy  $\omega$  to the total number of active MRs,

$$N_a(\epsilon, \omega) = X_a(\epsilon)p(\omega). \quad (3)$$

We suppose that the distribution function for potential energies of active MRs,  $p(\omega)$ , is strain-independent.

The ensemble of active meso-domains is described by the function  $n_a(t, \tau, \omega)$  that equals the number of active strands at time  $t$  (per unit mass) belonging to active MRs with potential energy  $\omega$  that have last been rearranged before instant  $\tau \in [0, t]$ . In particular,  $n_a(0, 0, \omega)$  is the number (per unit mass) of active strands in active MRs with potential energy  $\omega$  in a stress-free medium,

$$n_a(0, 0, \omega) = N_a(0, \omega), \quad (4)$$

and  $n_a(t, t, \omega)$  is the number (per unit mass) of active strands in active MRs with potential energy  $\omega$  in the deformed medium at time  $t$  (the initial time  $t = 0$  corresponds to the instant when external loads are applied to a specimen),

$$n_a(t, t, \omega) = N_a(\epsilon(t), \omega). \quad (5)$$

The amount

$$\left. \frac{\partial n_a}{\partial \tau}(t, \tau, \omega) \right|_{t=\tau} d\tau$$

equals the number (per unit mass) of dangling strands in active MRs with potential energy  $\omega$  that merge with the network within the interval  $[\tau, \tau + d\tau]$ , and the quantity

$$\frac{\partial n_a}{\partial \tau}(t, \tau, \omega) d\tau$$

is the number of these strands that have not detached from temporary junctions during the interval  $[\tau, t]$ . The number (per unit mass) of strands in active MRs that separate (for the first time) from the network within the interval  $[t, t + dt]$  reads

$$-\frac{\partial n_a}{\partial t}(t, 0, \omega) dt,$$

whereas the number (per unit mass) of strands in active MRs that merged with the network during the interval  $[\tau, \tau + d\tau]$  and, afterwards, separate from the network within the interval  $[t, t + dt]$  is given by

$$-\frac{\partial^2 n_a}{\partial t \partial \tau}(t, \tau, \omega) dt d\tau.$$

The rate of detachment,  $\Gamma$ , equals the ratio of the number of active strands that separate from the network per unit time to the current number of active strands. Applying this definition to active strands that merged with the network during the interval  $[\tau, \tau + d\tau]$  and separate from temporary junctions within the interval  $[t, t + dt]$ , we find that

$$\frac{\partial^2 n_a}{\partial t \partial \tau}(t, \tau, \omega) = -\Gamma(\epsilon(t), \omega) \frac{\partial n_a}{\partial \tau}(t, \tau, \omega). \quad (6)$$

Changes in the function  $n_a(t, 0, \omega)$  are governed by two processes at the micro-level: (i) detachment of active strands from temporary nodes, and (ii) transition of passive meso-domains into the active state under loading. The kinetic equation for this function reads

$$\frac{\partial n_a}{\partial t}(t, 0, \omega) = -\Gamma(\epsilon(t), \omega) n_a(t, 0, \omega) + \frac{\partial N_a}{\partial \epsilon}(\epsilon(t), \omega) \frac{d\epsilon}{dt}(t). \quad (7)$$

The solution of Eq. (7) with initial condition (4) is given by

$$\begin{aligned} n_a(t, 0, \omega) &= N_a(0, \omega) \exp\left[-\int_0^t \Gamma(\epsilon(s), \omega) ds\right] \\ &+ \int_0^t \frac{\partial N_a}{\partial \epsilon}(\epsilon(\tau), \omega) \frac{d\epsilon}{dt}(\tau) \exp\left[-\int_\tau^t \Gamma(\epsilon(s), \omega) ds\right] d\tau. \end{aligned} \quad (8)$$

It follows from Eq. (6) that

$$\frac{\partial n_a}{\partial \tau}(t, \tau, \omega) = \varphi(\tau, \omega) \exp\left[-\int_\tau^t \Gamma(\epsilon(s), \omega) ds\right], \quad (9)$$

where

$$\varphi(\tau, \omega) = \frac{\partial n_a}{\partial \tau}(t, \tau, \omega) \Big|_{t=\tau}. \quad (10)$$

To determine the function  $\varphi(t, \omega)$ , we use the identity

$$n_a(t, t, \omega) = n_a(t, 0, \omega) + \int_0^t \frac{\partial n_a}{\partial \tau}(t, \tau, \omega) d\tau. \quad (11)$$

Equations (5) and (11) imply that

$$n_a(t, 0, \omega) + \int_0^t \frac{\partial n_a}{\partial \tau}(t, \tau, \omega) d\tau = N_a(\epsilon(t), \omega). \quad (12)$$

Differentiating Eq. (12) with respect to time and using Eq. (10), we obtain

$$\varphi(t, \omega) + \frac{\partial n_a}{\partial t}(t, 0, \omega) + \int_0^t \frac{\partial^2 n_a}{\partial t \partial \tau}(t, \tau, \omega) d\tau = \frac{\partial N_a}{\partial \epsilon}(\epsilon(t), \omega) \frac{d\epsilon}{dt}(t).$$

This equality together with Eqs. (6), (7) and (11) results in

$$\begin{aligned}\varphi(t, \omega) &= \Gamma(\epsilon(t), \omega) \left[ n_a(t, 0, \omega) + \int_0^t \frac{\partial n_a}{\partial \tau}(t, \tau, \omega) d\tau \right] \\ &= \Gamma(\epsilon(t), \omega) n_a(t, t, \omega).\end{aligned}\quad (13)$$

Substituting expression (13) into Eq. (9) and using Eq. (5), we arrive at the formula

$$\frac{\partial n_a}{\partial \tau}(t, \tau, \omega) = \Gamma(\epsilon(t), \omega) N_a(\epsilon(t), \omega) \exp \left[ - \int_\tau^t \Gamma(\epsilon(s), \omega) ds \right]. \quad (14)$$

The kinetics of rearrangement of strands in active MRs is described by Eqs. (2), (3), (8) and (14). These relations are determined by (i) the distribution function  $p(\omega)$  for active MRs with various potential energies  $\omega$ , (ii) the function  $\Gamma_a(\epsilon)$  that characterizes the effect of strains on the attempt rate, and (iii) the function

$$\kappa_a(\epsilon) = \frac{X_a(\epsilon)}{X}, \quad (15)$$

that reflects mechanically-induced activation of passive MRs.

Rearrangement of strands in active MRs reflects the viscoelastic response of a semicrystalline polymer. The viscoplastic behavior is associated with the mechanically-induced slippage of junctions with respect to their positions in the bulk material.

Denote by  $\epsilon_u(t)$  the average strain induced by sliding of junctions between macromolecules (the subscript index “u” means that  $\epsilon_u(t)$  is associated with the residual strain in a specimen which is suddenly unloaded at instant  $t$ ). The elastic strain (that reflects elongation of active strands in a network) is denoted by  $\epsilon_e(t)$ . The functions  $\epsilon_e(t)$  and  $\epsilon_u(t)$  are connected with the macro-strain  $\epsilon(t)$  by the conventional formula

$$\epsilon(t) = \epsilon_e(t) + \epsilon_u(t). \quad (16)$$

We adopt the first order kinetics for slippage of junctions with respect to the bulk material, which implies that the increment of the viscoplastic strain,  $d\epsilon_u$ , induced by the growth of the macro-strain,  $\epsilon$ , by an increment,  $d\epsilon$ , is proportional to the absolute value of the stress  $\sigma$ ,

$$\frac{d\epsilon_u}{d\epsilon} = B|\sigma| \operatorname{sign}\left(\sigma \frac{d\epsilon}{dt}\right), \quad (17)$$

where the pre-factor  $B$  is a non-negative function of stress, strain and the strain rate,

$$B = B\left(\sigma, \epsilon, \frac{d\epsilon}{dt}\right).$$

The last multiplier in Eq. (17) determines the direction of the viscoplastic flow of junctions. It is convenient to present Eq. (17) in the form

$$\frac{d\epsilon_u}{dt}(t) = B\left(\sigma(t), \epsilon(t), \frac{d\epsilon}{dt}\right) |\sigma(t)| \operatorname{sign}\left[\sigma(t) \frac{d\epsilon}{dt}(t)\right] \frac{d\epsilon}{dt}(t), \quad \epsilon_u(0) = 0. \quad (18)$$

It follows from Eq. (18) that the rate of sliding vanishes when the strain is constant.



## 4 The strain energy density

Any strand is modelled as a linear elastic solid with the mechanical energy

$$w(t) = \frac{1}{2}\mu e^2(t),$$

where  $\mu$  is the average rigidity per strand and  $e$  is the strain from the stress-free state to the deformed state.

For strands belonging to passive meso-domains, the strain  $e$  coincides with  $\epsilon_e$ . Multiplying the strain energy per strand by the number of strands in passive MRs, we find the mechanical energy of meso-domains where rearrangement of chains is prevented by surrounding lamellae,

$$W_p(t) = \frac{1}{2}\mu X_p(\epsilon(t))\epsilon_e^2(t). \quad (19)$$

With reference to the conventional theory of temporary networks [31], we assume that stresses in dangling strands totally relax before these strands merge with the network. This implies that the reference (stress-free) state of a strand that merges with the network at time  $\tau$  coincides with the deformed state of the network at that instant. For active strands that have not been rearranged until time  $t$ , the strain  $e(t)$  coincides with  $\epsilon_e(t)$ , whereas for active strands that have last been merged with the network at time  $\tau \in [0, t]$ , the strain  $e(t, \tau)$  is given by

$$e(t, \tau) = \epsilon_e(t) - \epsilon_e(\tau).$$

Summing the mechanical energies of active strands belonging to active MRs with various potential energies,  $\omega$ , that were rearranged at various instants,  $\tau \in [0, t]$ , we find the mechanical energy of active meso-domains,

$$W_a(t) = \frac{1}{2}\mu \int_0^\infty d\omega \left\{ n_a(t, 0, \omega) \epsilon_e^2(t) + \int_0^t \frac{\partial n_a}{\partial \tau}(t, \tau, \omega) [\epsilon_e(t) - \epsilon_e(\tau)]^2 d\tau \right\}. \quad (20)$$

The mechanical energy per unit mass of a polymer reads

$$W(t) = W_a(t) + W_p(t).$$

Substituting expressions (19) and (20) into this equality and using Eq. (16), we arrive at the formula

$$\begin{aligned} W(t) = & \frac{1}{2}\mu \left\{ X_p(\epsilon(t)) (\epsilon(t) - \epsilon_u(t))^2(t) + \int_0^\infty d\omega \left[ n_a(t, 0, \omega) (\epsilon(t) - \epsilon_u(t))^2 \right. \right. \\ & \left. \left. + \int_0^t \frac{\partial n_a}{\partial \tau}(t, \tau, \omega) \left( (\epsilon(t) - \epsilon_u(t)) - (\epsilon(\tau) - \epsilon_u(\tau)) \right)^2 d\tau \right] \right\}. \end{aligned} \quad (21)$$

Differentiation of Eq. (21) with respect to time results in

$$\frac{dW}{dt}(t) = \mu A(t) \left[ \frac{d\epsilon}{dt}(t) - \frac{d\epsilon_u}{dt}(t) \right] + \frac{1}{2}\mu A_0(t), \quad (22)$$

where

$$\begin{aligned}
A(t) &= X_p(\epsilon(t))[\epsilon(t) - \epsilon_u(t)] + \int_0^\infty d\omega \left\{ n_a(t, 0, \omega) [\epsilon(t) - \epsilon_u(t)] \right. \\
&\quad \left. + \int_0^t \frac{\partial n_a}{\partial \tau}(t, \tau, \omega) [(\epsilon(t) - \epsilon_u(t)) - (\epsilon(\tau) - \epsilon_u(\tau))] d\tau \right\}, \\
A_0(t) &= \frac{\partial X_p}{\partial \epsilon}(\epsilon(t)) \frac{d\epsilon}{dt}(t) [\epsilon(t) - \epsilon_u(t)]^2 + \int_0^\infty d\omega \left\{ \frac{\partial n_a}{\partial t}(t, 0, \omega) [\epsilon(t) - \epsilon_u(t)]^2 \right. \\
&\quad \left. + \int_0^t \frac{\partial^2 n_a}{\partial t \partial \tau}(t, \tau, \omega) [(\epsilon(t) - \epsilon_u(t)) - (\epsilon(\tau) - \epsilon_u(\tau))]^2 d\tau \right\}. \tag{23}
\end{aligned}$$

Bearing in mind Eqs. (5) and (11), we transform the first equality in Eq. (23) as follows:

$$\begin{aligned}
A(t) &= \left[ X_p(\epsilon(t)) + \int_0^\infty N_a(\epsilon(t), \omega) d\omega \right] [\epsilon(t) - \epsilon_u(t)] \\
&\quad - \int_0^\infty d\omega \int_0^t \frac{\partial n_a}{\partial \tau}(t, \tau, \omega) [\epsilon(\tau) - \epsilon_u(\tau)] d\tau.
\end{aligned}$$

This formula together with Eqs. (1) and (3) implies that

$$A(t) = X[\epsilon(t) - \epsilon_u(t)] - \int_0^\infty d\omega \int_0^t \frac{\partial n_a}{\partial \tau}(t, \tau, \omega) [\epsilon(\tau) - \epsilon_u(\tau)] d\tau. \tag{24}$$

Substitution of expressions (6) and (7) into the second equality in Eq. (23) yields

$$A_0(t) = \left[ \frac{\partial X_p}{\partial \epsilon}(\epsilon(t)) + \int_0^\infty \frac{\partial N_a}{\partial \epsilon}(\epsilon(t), \omega) d\omega \right] \frac{d\epsilon}{dt}(t) [\epsilon(t) - \epsilon_u(t)]^2 - A_1(t), \tag{25}$$

where

$$\begin{aligned}
A_1(t) &= \int_0^\infty \Gamma(\epsilon(t), \omega) d\omega \left\{ n_a(t, 0, \omega) [\epsilon(t) - \epsilon_u(t)]^2 \right. \\
&\quad \left. + \int_0^t \frac{\partial n_a}{\partial \tau}(t, \tau, \omega) [(\epsilon(t) - \epsilon_u(t)) - (\epsilon(\tau) - \epsilon_u(\tau))]^2 d\tau \right\}. \tag{26}
\end{aligned}$$

It follows from Eqs. (1), (3) and (25) that

$$A_0(t) = -A_1(t).$$

This equality together with Eq. (22) results in

$$\frac{dW}{dt}(t) = \mu \left[ A(t) \frac{d\epsilon}{dt}(t) - \frac{1}{2} (A_1(t) + A_2(t)) \right], \tag{27}$$

where

$$A_2(t) = 2A(t) \frac{d\epsilon_u}{dt}(t). \tag{28}$$

## 5 Constitutive equations

For uniaxial loading with small strains at the reference temperature  $T_0$ , the Clausius-Duhem inequality reads [39]

$$T_0 \frac{dQ}{dt}(t) = -\frac{dW}{dt}(t) + \frac{1}{\rho} \sigma(t) \frac{d\epsilon}{dt}(t) \geq 0, \quad (29)$$

where  $\rho$  is mass density, and  $Q$  is the entropy production per unit mass. Substitution of expression (27) into Eq. (29) implies that

$$T_0 \frac{dQ}{dt}(t) = \frac{1}{\rho} [\sigma(t) - \rho \mu A(t)] \frac{d\epsilon}{dt}(t) + \frac{1}{2} [A_1(t) + A_2(t)] \geq 0. \quad (30)$$

Because Eq. (30) is to be fulfilled for an arbitrary program of straining,  $\epsilon = \epsilon(t)$ , the expression in the first square brackets vanishes. This assertion together with Eq. (24) results in the stress-strain relation

$$\begin{aligned} \sigma(t) &= \rho \mu A(t) \\ &= E \left\{ [\epsilon(t) - \epsilon_u(t)] - \frac{1}{X} \int_0^\infty d\omega \int_0^t \frac{\partial n_a}{\partial \tau}(t, \tau, \omega) [\epsilon(\tau) - \epsilon_u(\tau)] d\tau \right\}, \end{aligned} \quad (31)$$

where

$$E = \rho \mu X$$

is an analog of the Young modulus. It follows from Eqs. (18), (28) and (31) that

$$A_2(t) = \frac{2}{\rho \mu} B\left(\sigma(t), \epsilon(t), \frac{d\epsilon}{dt}(t)\right) \sigma^2(t) \left| \frac{d\epsilon}{dt}(t) \right|. \quad (32)$$

According to Eqs. (26) and (32), the functions  $A_1(t)$  and  $A_2(t)$  are non-negative for an arbitrary program of loading, which, together with Eq. (31), implies that the Clausius-Duhem inequality (30) is satisfied.

Substitution of Eqs. (3), (14) and (15) into Eq. (31) results in the constitutive equation

$$\begin{aligned} \sigma(t) &= E \left\{ [\epsilon(t) - \epsilon_u(t)] - \kappa_a(\epsilon(t)) \int_0^\infty p(\omega) d\omega \right. \\ &\quad \left. \times \int_0^t \Gamma(\epsilon(t), \omega) \exp\left[-\int_\tau^t \Gamma(\epsilon(s), \omega) ds\right] [\epsilon(\tau) - \epsilon_u(\tau)] d\tau \right\}. \end{aligned} \quad (33)$$

Given functions  $p(\omega)$ ,  $\Gamma_a(\epsilon)$  and  $\kappa_a(\epsilon)$ , the time-dependent response of a semicrystalline polymer at isothermal uniaxial loading with small strains is determined by Eqs. (2), (18) and (33). For a standard relaxation test with the longitudinal strain  $\epsilon^0$ ,

$$\epsilon(t) = \begin{cases} 0, & t < 0, \\ \epsilon^0, & t \geq 0, \end{cases}$$

these equations imply that

$$\sigma(t, \epsilon^0) = E(\epsilon^0 - \epsilon_u^0) \left\{ 1 - \kappa_a(\epsilon^0) \int_0^\infty p(\omega) \left[ 1 - \exp(-\Gamma_a(\epsilon^0) \exp(-\omega)t) \right] d\omega \right\},$$

where  $\epsilon_u^0$  is the strain induced by sliding of junctions. Introducing the notation

$$C_1(\epsilon^0) = E(\epsilon^0 - \epsilon_u^0), \quad C_2(\epsilon^0) = E(\epsilon^0 - \epsilon_u^0)\kappa_a(\epsilon^0), \quad (34)$$

we present this equality as follows:

$$\sigma(t, \epsilon^0) = C_1(\epsilon^0) - C_2(\epsilon^0) \int_0^\infty p(\omega) \left[ 1 - \exp(-\Gamma_a(\epsilon^0) \exp(-\omega)t) \right] d\omega. \quad (35)$$

To fit experimental data, we adopt the random energy model [40] with

$$p(\omega) = p_0 \exp\left[-\frac{(\omega - \Omega)^2}{2\Sigma^2}\right] \quad (\omega \geq 0), \quad p(\omega) = 0 \quad (\omega < 0), \quad (36)$$

where  $\Omega$  and  $\Sigma$  are adjustable parameters, and the pre-factor  $p_0$  is determined by the condition

$$\int_0^\infty p(\omega) d\omega = 1. \quad (37)$$

Given a strain  $\epsilon^0$ , Eqs. (35) and (36) are determined by 5 material constants:

1. the average potential energy for rearrangement of strands  $\Omega$ ,
2. the standard deviation of distribution of potential energies  $\Sigma$ ,
3. the attempt rate for separation of strands in active MRs from their junctions  $\Gamma_a$ ,
4. the coefficients  $C_1$  and  $C_2$ .

Our purpose now is to find these parameters by fitting experimental data.

## 6 Fitting of observations

We begin with matching the relaxation curve measured at the strain  $\epsilon_8 = 0.025$ . Because the rate of rearrangement,  $\Gamma_a$ , and the average activation energy,  $\Omega$ , are mutually dependent [Eqs. (35) and (36) imply that the growth of  $\Omega$  results in an increase in  $\Gamma_a$ ], we set  $\Gamma_a = 1$  s and approximate the relaxation curve by using 4 experimental constants:  $\Omega$ ,  $\Sigma$ ,  $C_1$  and  $C_2$ . To find these quantities, we fix the intervals  $[0, \Omega_{\max}]$  and  $[0, \Sigma_{\max}]$ , where the “best-fit” parameters  $\Omega$  and  $\Sigma$  are assumed to be located, and divide these intervals into  $J$  subintervals by the points  $\Omega_i = i\Delta_\Omega$  and  $\Sigma_j = j\Delta_\Sigma$  ( $i, j = 1, \dots, J$ ) with  $\Delta_\Omega = \Omega_{\max}/J$ ,  $\Delta_\Sigma = \Sigma_{\max}/J$ . For any pair,  $\{\Omega_i, \Sigma_j\}$ , the integral in Eq. (35) is evaluated numerically (by Simpson’s method with 200 points and the step  $\Delta_\omega = 0.1$ ). The pre-factor  $p_0$  is determined by Eq. (37). The coefficients  $C_1 = C_1(i, j)$  and  $C_2 = C_2(i, j)$  that minimize the function

$$\mathcal{J}(i, j) = \sum_{t_m} \left[ \sigma_{\text{exp}}(t_m) - \sigma_{\text{num}}(t_m) \right]^2, \quad (38)$$

where the sum is calculated over all experimental points  $t_m$ , are found by the least-squares method. The stress  $\sigma_{\text{exp}}$  in Eq. (38) is measured in the relaxation test, whereas

the quantity  $\sigma_{\text{num}}$  is given by Eq. (35). The “best-fit” parameters  $\Omega$  and  $\Sigma$  minimize the function  $\mathcal{J}$  on the set

$$\{\Omega_i, \Sigma_j \quad (i, j = 1, \dots, J)\}.$$

After determining the “best-fit” constants,  $\Omega_i$  and  $\Sigma_j$ , this procedure is repeated for the new intervals  $[\Omega_{i-1}, \Omega_{i+1}]$  and  $[\Sigma_{j-1}, \Sigma_{j+1}]$  to ensure good accuracy of fitting. Figure 2 demonstrates fair agreement between the experimental data and the results of numerical simulation with  $\Omega = 5.03$  and  $\Sigma = 3.05$ .

To approximate relaxation curves at other strains,  $\epsilon_k$ , we fix the constants  $\Omega$  and  $\Sigma$  found by matching experimental data at  $\epsilon_8$  and fit every relaxation curve by using 3 adjustable parameters:  $\Gamma_a$ ,  $C_1$  and  $C_2$ . To find these quantities, an algorithm is applied similar to that employed to match the relaxation curve at  $\epsilon_8 = 0.025$ . We fix the interval  $[0, \Gamma_{\text{max}}]$ , where the “best-fit” attempt rate  $\Gamma_a$  is supposed to be located, and divide this interval into  $J$  subintervals by the points  $\Gamma_i = i\Delta_\Gamma$  ( $i = 1, \dots, J$ ) with  $\Delta_\Gamma = \Gamma_{\text{max}}/J$ . For any  $\Gamma_i$ , we calculate the integral in Eq. (35) numerically and find the coefficients  $C_1 = C_1(i)$  and  $C_2 = C_2(i)$  minimizing the function (38) by the least-squares method. The “best-fit” attempt rate is determined from the condition of minimum for the function  $\mathcal{J}$  on the set  $\{\Gamma_i \quad (i = 1, \dots, J)\}$ . After finding the “best-fit” value,  $\Gamma_i$ , this procedure is repeated for the new interval  $[\Gamma_{i-1}, \Gamma_{i+1}]$  to ensure an acceptable accuracy of fitting. Figures 2 to 4 show good agreement between the observations and the results of numerical analysis.

For any longitudinal strain  $\epsilon_k$ , the attempt rate,  $\Gamma_a(\epsilon_k)$ , is determined by matching an appropriate relaxation curve. The fraction of active MRs,  $\kappa_a(\epsilon_k)$ , is found from Eq. (34),

$$\kappa_a(\epsilon_k) = \frac{C_2(\epsilon_k)}{C_1(\epsilon_k)}.$$

These quantities are plotted versus strain  $\epsilon$  in Figures 5 and 6. The experimental data are approximated by the phenomenological equations

$$\log \Gamma_a = \gamma_0 + \gamma_1 \epsilon, \quad \kappa_a = k_0 + k_1 \epsilon, \quad (39)$$

where the coefficients  $\gamma_i$  and  $k_i$  are found by the least-squares method. Figures 5 and 6 reveal two different regimes of the nonlinear viscoelastic behavior of polypropylene. In the region of relatively small strains (less than  $\epsilon_* = 0.02$ ), the quantities  $\log \Gamma_a$  and  $\kappa_a$  increase linearly with strain,  $\epsilon$ . In the region of strains exceeding the threshold value,  $\epsilon_*$ , the attempt rate grows rather weakly, and the fraction of active MRs remains constant. This observation implies that the free-volume theory may be applied to the description of the nonlinear viscoelastic response of polypropylene at relatively small strains only. When strains exceed the threshold value,  $\epsilon_*$ , relaxation of longitudinal stresses becomes strain-independent.

This conclusion results in two questions of interest:

1. What is a micro-mechanism for transition from the nonlinear (strain-dependent) to the linear (strain-independent) viscoelastic behavior of isotactic polypropylene at the threshold strain,  $\epsilon_*$ .

2. Whether other semicrystalline polymers demonstrate the nonlinear time-dependent response in a limited range of strains only, i.e., whether relaxation of stresses in semicrystalline polymers (unlike amorphous glassy polymers) becomes strain-independent at threshold strains,  $\epsilon_*$ , that are noticeably lower than the yield strain,  $\epsilon_y$ .

These issues will be the subject of a subsequent study.

## 7 Concluding remarks

Constitutive equations have been derived for the time-dependent behavior of semicrystalline polymers at isothermal loading with small strains. To develop stress-strain relations, a version of the mean-field approach is employed: a complicated micro-structure of isotactic polypropylene is replaced by an equivalent transient network of macromolecules bridged by junctions (physical cross-links, entanglements and crystalline lamellae). The network is assumed to be strongly inhomogeneous, and it is thought of as an ensemble of meso-regions with various potential energies for separation of strands from temporary nodes.

The viscoelastic response of a semicrystalline polymer is ascribed to the processes of detachment and reformation of chains in active meso-domains. Rearrangement of active strands is modelled as a thermo-mechanically activated process whose rate obeys the Eyring formula.

The viscoplastic response is described by slippage of junctions with respect to their positions in the bulk material. The rate of sliding of junctions is assumed to be proportional to the macro-stress in a specimen.

The mechanical energy is determined as the sum of the strain energies of active strands. Constitutive equations are derived by using the laws of thermodynamics. These relations are applied to study relaxation of longitudinal stresses at uniaxial tension of specimens.

A series of relaxation tests have been performed on isotactic polypropylene at room temperature. Adjustable parameters in the stress-strain equations are found by fitting observations. The following conclusions are drawn from the analysis of experimental data:

1. Despite a complicated morphology of isotactic polypropylene, its time-dependent response is rheologically simple in the sense that the relaxation spectrum (which is determined by distribution function,  $p(\omega)$ , for potential energies of active MRs) is not affected by mechanical factors.
2. Two regimes of the nonlinear viscoelastic behavior of polypropylene are observed. At relatively small strains (less than the threshold value  $\epsilon_* = 0.02$ ), the attempt rate,  $\Gamma_a$ , and the fraction of active MRs,  $\kappa_a$ , increase with strain,  $\epsilon$ , in agreement with the free-volume concept. When the strain,  $\epsilon$ , exceeds its threshold value,  $\epsilon_*$ , the attempt rate,  $\Gamma_a$ , grows with strain rather weakly, while the fraction of active MRs,  $\kappa_a$ , remains constant.

## References

- [1] I.M. Ward and J.M. Wolfe, The non-linear mechanical behaviour of polypropylene fibers under complex loading programmes. *J. Mech. Phys. Solids* **14**, 131 (1966).
- [2] I.M. Ward and D.W. Hadley, *An Introduction to the Mechanical Properties of Solid Polymers*. Wiley, New York (1993).
- [3] J. Smart and J.G. Williams, A comparison of single-integral non-linear viscoelasticity theories. *J. Mech. Phys. Solids* **20**, 313 (1972).
- [4] T. Ariyama, Cyclic deformation and relaxation characteristics in polypropylene. *Polym. Eng. Sci.* **33**, 18 (1993).
- [5] T. Ariyama, Stress relaxation behavior after cyclic preloading in polypropylene. *Polym. Eng. Sci.* **33**, 1494 (1993).
- [6] T. Ariyama, Viscoelastic-plastic behaviour with mean strain changes in polypropylene. *J. Mater. Sci.* **31**, 4127 (1996).
- [7] T. Ariyama, Y. Mori, and K. Kaneko, Tensile properties and stress relaxation of polypropylene at elevated temperatures. *Polym. Eng. Sci.* **37**, 81 (1997).
- [8] F.-J. Wortmann and K.V. Schulz, Non-linear viscoelastic performance of Nomex, Kevlar and polypropylene fibres in a single-step stress relaxation test: 1. Experimental data and principles of analysis. *Polymer* **35**, 2108 (1994).
- [9] F.-J. Wortmann and K.V. Schulz, Non-linear viscoelastic performance of Nomex, Kevlar and polypropylene fibres in a single step stress relaxation test: 2. Moduli, viscosities and isochronal stress/strain curves. *Polymer* **36**, 2363 (1995).
- [10] N.K. Dutta and G.H. Edward, Generic relaxation spectra of solid polymers. 1. Development of spectral distribution model and its application to stress relaxation of polypropylene. *J. Appl. Polym. Sci.* **66**, 1101 (1997).
- [11] B.E. Read and P.E. Tomlins, Time-dependent deformation of polypropylene in response to different stress histories. *Polymer* **38**, 4617 (1997).
- [12] E. Andreassen, Stress relaxation of polypropylene fibres with various morphologies. *Polymer* **40**, 3909 (1999).
- [13] M.A. Lopez-Manchado and M. Arroyo, Thermal and dynamic mechanical properties of polypropylene and short organic fiber composites. *Polymer* **41**, 7761 (2000).
- [14] A.M.C. Souza and N.R. Demarquette, Influence of composition on the linear viscoelastic behavior and morphology of PP/HDPE blends. *Polymer* **43**, 1313 (2002).
- [15] G. Gallego Ferrer, M. Salmeron Sanchez, E. Verdu Sanchez, F. Romero Colomer, and J.L. Gomez Ribelles, Blends of styrene-butadiene-styrene triblock copolymer and isotactic polypropylene: morphology and thermomechanical properties. *Polym. Int.* **49**, 853 (2000).

- [16] R. Seguela, E. Staniek, B. Escaig, and B. Fillon, Plastic deformation of polypropylene in relation to crystalline structure. *J. Appl. Polym. Sci.* **71**, 1873 (1999).
- [17] G. Coulon, G. Castelein, and C. G'Sell, Scanning force microscopic investigation of plasticity and damage mechanisms in polypropylene spherulites under simple shear. *Polymer* **40**, 95 (1998).
- [18] T. Labour, L. Ferry, C. Gauthier, P. Hajji, and G. Vigier,  $\alpha$ - and  $\beta$ - crystalline forms of isotactic polypropylene investigated by nanoindentation. *J. Appl. Polym. Sci.* **74**, 195 (1999).
- [19] X.C. Zhang, M.F. Butler, and R.E. Cameron, The relationships between morphology, irradiation and the ductile–brittle transition of isotactic polypropylene. *Polym. Int.* **48**, 1173 (1999).
- [20] J.S. Bergstrom, S.M. Kurtz, C.M. Rimnac, and A.A. Edidin, Constitutive modeling of ultra-high molecular weight polyethylene under large-deformation and cyclic loading conditions. *Biomaterials* **23**, (2002).
- [21] K.-H. Nitta and M. Takayanagi, Role of tie molecules in the yielding deformation of isotactic polypropylene. *J. Polym. Sci. B: Polym. Phys.* **37**, 357 (1999).
- [22] K.-H. Nitta and M. Takayanagi, Tensile yield of isotactic polypropylene in terms of a lamellar-cluster model. *J. Polym. Sci. B: Polym. Phys.* **38**, 1037 (2000).
- [23] R.W. Meyer and L.A. Pruitt, The effect of cyclic true strain on the morphology, structure, and relaxation behavior of ultra high molecular weight polyethylene. *Polymer* **42**, 5293 (2001).
- [24] J. Sweeney and I.M. Ward, The modelling of multiaxial necking in polypropylene using a sliplink-crosslink theory. *J. Rheol.* **39**, 861 (1995).
- [25] J. Sweeney and I.M. Ward, A constitutive law for large deformations of polymers at high temperatures. *J. Mech. Phys. Solids* **44**, 1033 (1996).
- [26] P.G. Llana and M.C. Boyce, Finite strain behavior of poly(ethylene terephthalate) above the glass transition temperature. *Polymer* **40**, 6729 (1999).
- [27] M.C. Boyce, S. Socrate, and P.G. Llana, Constitutive model for the finite deformation stress-strain behavior of poly(ethylene terephthalate) above the glass transition. *Polymer* **41**, 2183 (2000).
- [28] M.S. Green and A.V. Tobolsky, A new approach to the theory of relaxing polymeric media. *J. Chem. Phys.* **14**, 80 (1946).
- [29] M. Yamamoto, The visco-elastic properties of network structure. 1. General formalism. *J. Phys. Soc. Japan* **11**, 413 (1956).
- [30] A.S. Lodge, Constitutive equations from molecular network theories for polymer solutions. *Rheol. Acta* **7**, 379 (1968).



- [31] F. Tanaka and S.F. Edwards, Viscoelastic properties of physically cross-linked networks. Transient network theory. *Macromolecules* **25**, 1516 (1992).
- [32] A.S. Krausz and H. Eyring, *Deformation Kinetics*. Wiley, New York (1975).
- [33] M.B.M. Mangion, J.Y. Cavaille, and J. Perez, A molecular theory for the sub- $T_g$  plastic mechanical response of amorphous polymers. *Phil. Magazine* **A66**, 773 (1992).
- [34] W.G. Knauss and I.J. Emri, Volume change and the nonlinearly thermoviscoelastic constitution of polymers. *Polym. Eng. Sci.* **27**, 86 (1987).
- [35] G.U. Losi and W.G. Knauss, Free volume theory and nonlinear thermoviscoelasticity. *Polym. Eng. Sci.* **32**, 542 (1992).
- [36] N.P. O'Dowd and W.G. Knauss, Time dependent large principal deformation of polymers. *J. Mech. Phys. Solids* **43**, 771 (1995).
- [37] M.K. Chengalva, V.H. Kenner, and C.H. Popelar, An evaluation of a free volume representation for viscoelastic properties. *Int. J. Solids Structures* **32**, 847 (1995).
- [38] B. Wunderlich, *Macromolecular Physics*. Vol. 3, *Crystal Melting*. Academic Press, New York (1980).
- [39] P. Haupt, *Continuum Mechanics and Theory of Materials*. Springer, Berlin (2000).
- [40] J.C. Dyre, Energy master equation: a low temperature approximation to Bässler's random-walk model. *Phys. Rev. B* **51**, 12276 (1995).

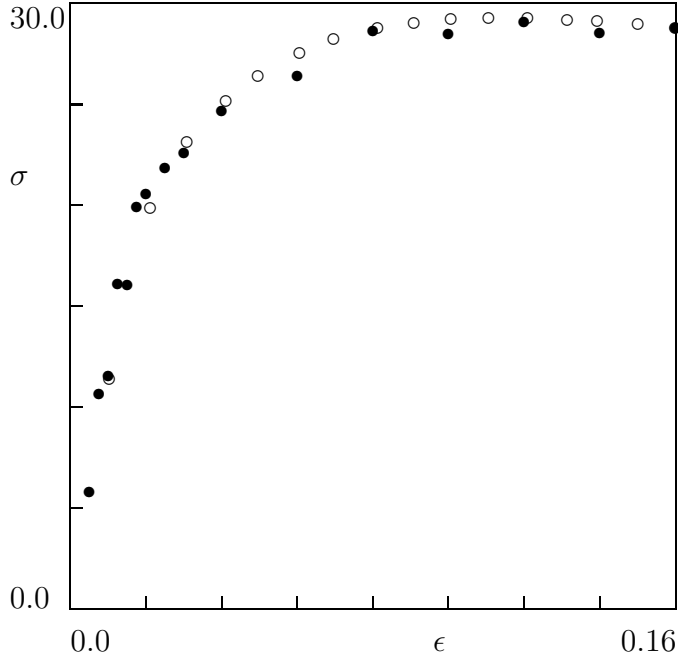


Figure 1: The longitudinal stress  $\sigma$  MPa versus strain  $\epsilon$ . Unfilled circles: experimental data in a tensile test with the cross-head speed 5 mm/min. Filled circles: experimental data at the beginnings of relaxation tests

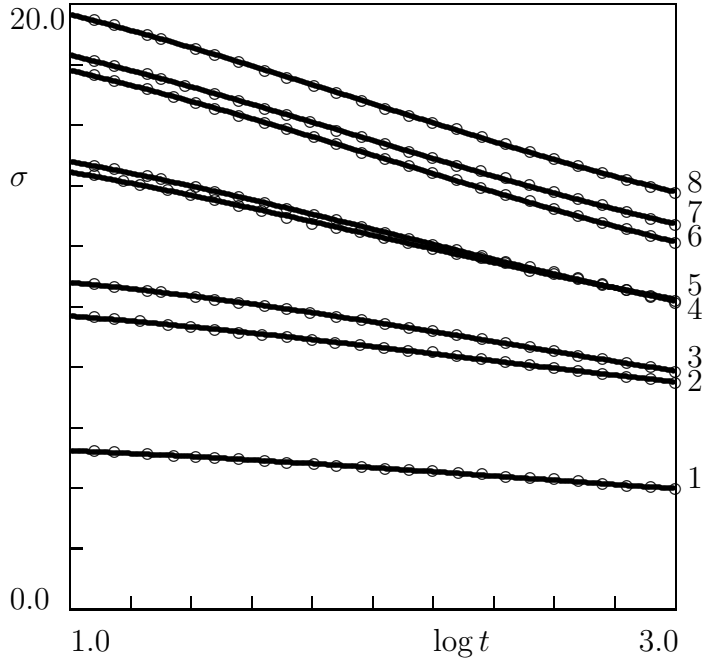


Figure 2: The longitudinal stress  $\sigma$  MPa versus time  $t$  s in a tensile relaxation test at a strain  $\epsilon$ . Circles: experimental data. Solid lines: results of numerical simulation. Curve 1:  $\epsilon = 0.005$ ; curve 2:  $\epsilon = 0.0075$ ; curve 3:  $\epsilon = 0.010$ ; curve 4:  $\epsilon = 0.0125$ ; curve 5:  $\epsilon = 0.015$ ; curve 6:  $\epsilon = 0.0175$ ; curve 7:  $\epsilon = 0.020$ ; curve 8:  $\epsilon = 0.025$

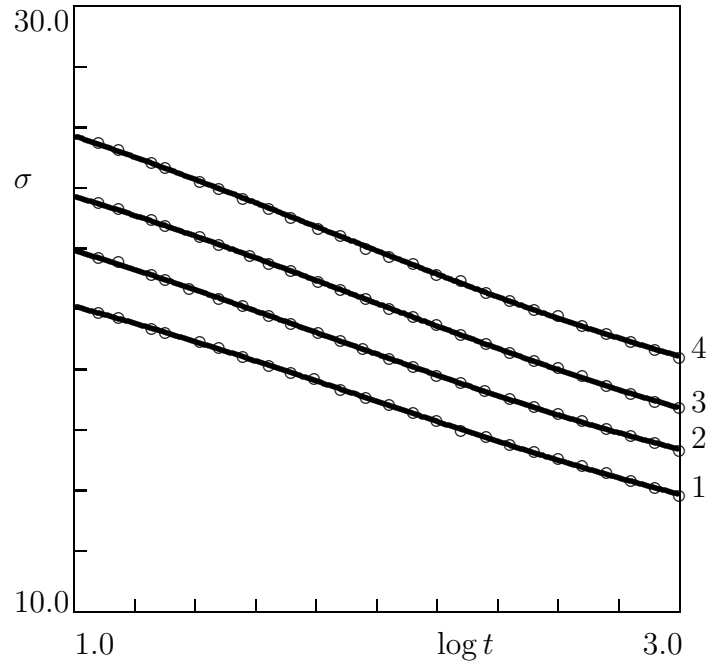


Figure 3: The longitudinal stress  $\sigma$  MPa versus time  $t$  s in a tensile relaxation test at a strain  $\epsilon$ . Circles: experimental data. Solid lines: results of numerical simulation. Curve 1:  $\epsilon = 0.03$ ; curve 2:  $\epsilon = 0.04$ ; curve 3:  $\epsilon = 0.06$ ; curve 4:  $\epsilon = 0.08$

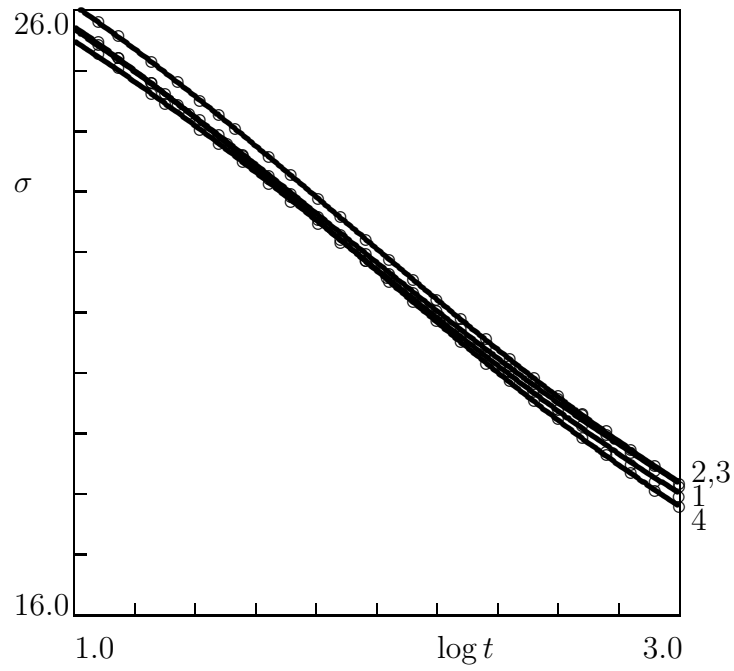


Figure 4: The longitudinal stress  $\sigma$  MPa versus time  $t$  s in a tensile relaxation test at a strain  $\epsilon$ . Circles: experimental data. Solid lines: results of numerical simulation. Curve 1:  $\epsilon = 0.10$ ; curve 2:  $\epsilon = 0.12$ ; curve 3:  $\epsilon = 0.14$ ; curve 4:  $\epsilon = 0.16$

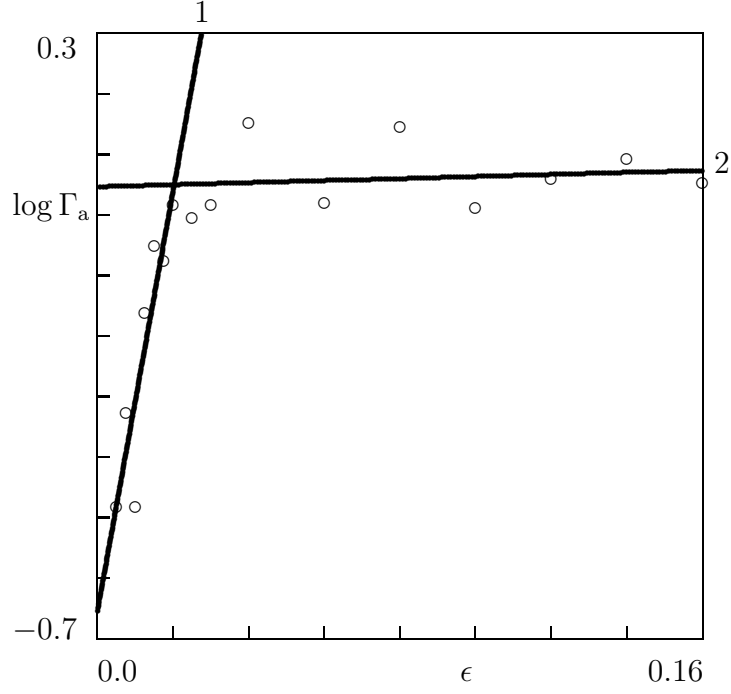


Figure 5: The attempt rate  $\Gamma_a \text{ s}^{-1}$  versus strain  $\epsilon$  in tensile relaxation tests. Circles: treatment of observations. Solid lines: approximation of the experimental data by Eq. (39). Curve 1:  $\gamma_0 = -0.66$ ,  $\gamma_1 = 34.73$ ; curve 2:  $\gamma_0 = 0.05$ ,  $\gamma_1 = 0.17$

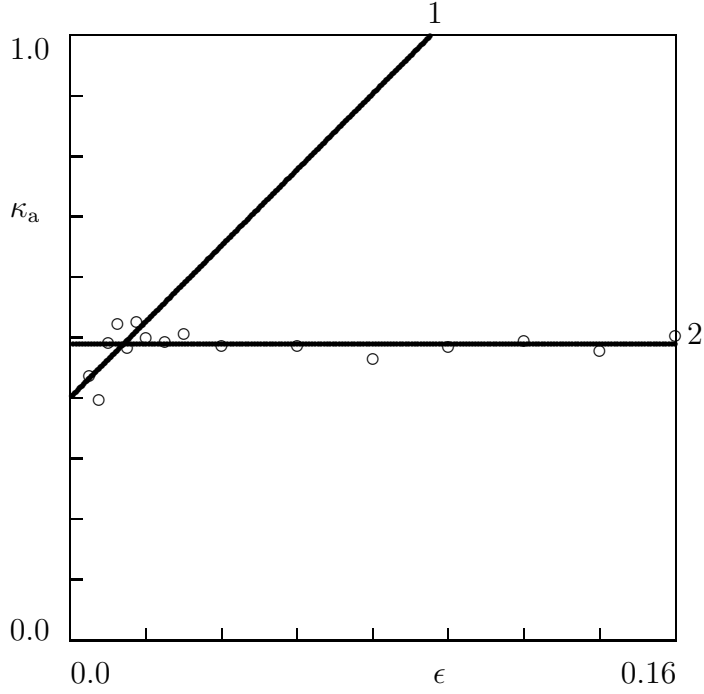


Figure 6: The fraction of active MRs  $\kappa_a$  versus strain  $\epsilon$  in tensile relaxation tests. Circles: treatment of observations. Solid lines: approximation of the experimental data by Eq. (39). Curve 1:  $k_0 = 0.40$ ,  $k_1 = 6.28$ ; curve 2:  $k_0 = 0.49$ ,  $k_1 = 0.0$